Nucleosomal Fluctuations Govern the Transcription Dynamics of RNA Polymerase II

Courtney Hodges,[1]* Lacramioara Bintu,[2]* Lucyna Lubkowska,[3] Mikhail Kashlev,[3] Carlos Bustamante[1,2,4]†

RNA polymerase II (Pol II) must overcome the barriers imposed by nucleosomes during transcription elongation. We have developed an optical tweezers assay to follow individual Pol II complexes as they transcribe nucleosomal DNA. Our results indicate that the nucleosome behaves as a fluctuating barrier that locally increases pause density, slows pause recovery, and reduces the apparent pause-free velocity of Pol II. The polymerase, rather than actively separating DNA from histones, functions instead as a ratchet that rectifies nucleosomal fluctuations. We also obtained direct evidence that transcription through a nucleosome involves transfer of the core histones behind the transcribing polymerase via a transient DNA loop. The interplay between polymerase dynamics and nucleosome fluctuations provides a physical basis for the regulation of eukaryotic transcription.

During transcription elongation in eukaryotes, RNA polymerase II (Pol II) must overcome the transcriptional barriers imposed by nucleosomes in chromatin. In vitro, a single nucleosome is sufficient to halt or greatly slow transcription by Pol II (*1*–*5*), and factors that restrict transcriptional backtracking relieve nucleosome-induced pauses and arrests, which suggests that the influence of the nucleosome is mediated through polymerase backtracking (*4*). Pol II also affects nucleosomal dynamics: Depletion and turnover of histones are seen in actively transcribed genes in vivo (*6*, *7*), and histones are often transferred behind transcribing polymerases in vitro (*2*). However, the mechanisms underlying the mutual influence between nucleosome and polymerase are not well understood.

Here, a dual-trap optical tweezers assay revealed real-time trajectories of individual Pol II complexes as they transcribed through single nucleosomes. A tether was created between two trapped beads—one attached to a stalled polymerase, the other to the upstream DNA (Fig. 1A) (*8*). Addition of ribonucleotide triphosphates induced the polymerase to move toward the nucleosomal positioning sequence (NPS), causing the force between the two beads to decrease. The position of the polymerase was calculated by fitting the measured force to the worm-like chain formula of DNA elasticity (*9*).

In the absence of a nucleosome, polymerases generally proceeded to the end of the DNA template, interrupted only by a few short pauses (Fig. 1B, black traces). When we preloaded a single core nucleosome onto the template, Pol II showed pronounced changes in its dynamics, ranging from one or two pauses to complete arrest at the nucleosome (Fig. 1B, colored traces). We observed a marked decrease in the frequency of nucleosomal arrest with increasing ionic strength (Fig. 1, C to E) (*2*, *5*). The influence of ionic strength on arrest parallels a decrease in the mechanical stability of the nucleosome with salt, but does not correlate with changes in the dynamics of transcription on bare DNA (*8*). Because a majority of polymerases were able to pass the nucleosome at 300 mM KCl, we conducted more detailed studies of nucleosomal transcription at this ionic strength.

To establish whether the nucleosome affected pause entry, we counted all pauses of at least 2 s and recorded their positions on the DNA template (Fig. 2A). The nucleosome locally increased the probability of Pol II to enter a paused state by a factor of ~3, from 0.0079 ± 0.002 bp^{-1} on bare DNA (bp, base pairs) to a peak of 0.022 ± 0.004 bp^{-1} at the nucleosome. The effect on pause density was strongest before the polymerase reached the dyad axis of the nucleosome (Fig. 2A) (*5*). Pause durations at the nucleosome were highly variable among trajectories and within a given trajectory. A comparison of the cumulative distributions of the pause durations shows that the nucleosome biases the polymerase toward longer pauses ($P < 0.001$, Fig. 2B), increasing the me-

[1]Jason L. Choy Laboratory of Single-Molecule Biophysics and Biophysics Graduate Group, University of California, Berkeley, CA 94720, USA. [2]Department of Physics, University of California, Berkeley, CA 94720, USA. [3]NCI Center for Cancer Research, National Cancer Institute–Frederick Cancer Research and Development Center, Frederick, MD 21702, USA. [4]Howard Hughes Medical Institute, Department of Chemistry and Molecular and Cell Biology, University of California, Berkeley, CA 94720, USA.

*These authors contributed equally to this work.
†To whom correspondence should be addressed. E-mail: carlos@alice.berkeley.edu

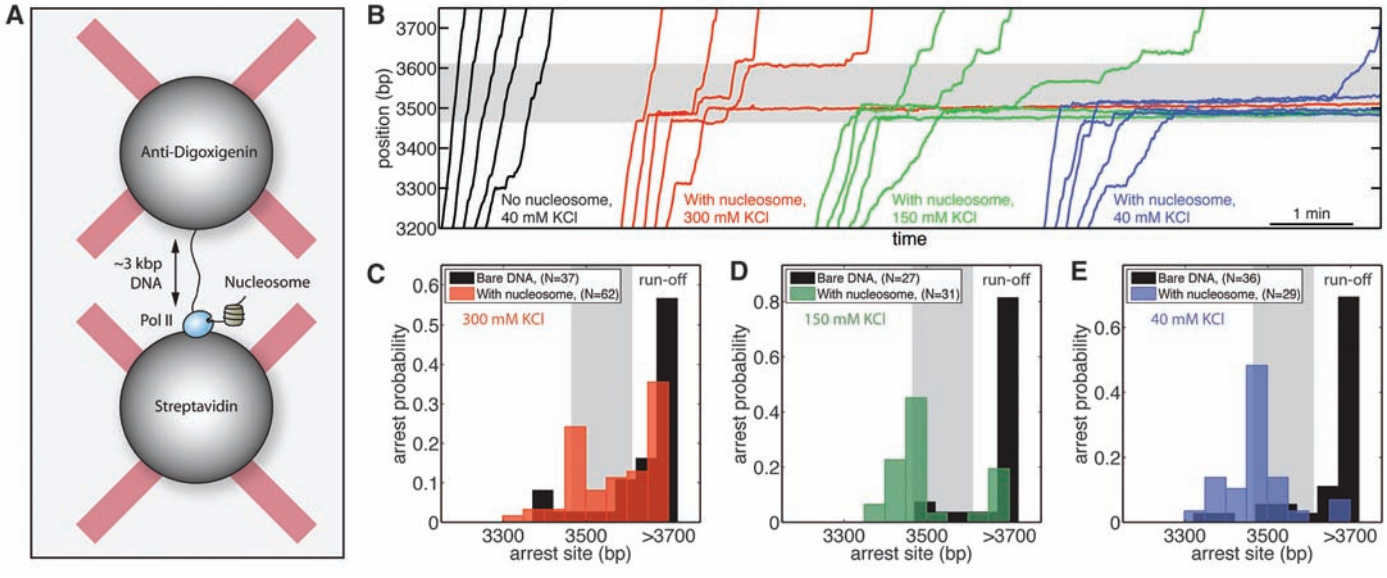

Fig. 1. Transcription through a nucleosome. (**A**) Geometry for the dual-trap optical tweezers experiments. (**B**) Representative trajectories of individual transcribing polymerases with or without the nucleosome at different ionic strengths. (**C** to **E**) Probability of arrest or termination as a function of polymerase position on the DNA template at 300, 150, and 40 mM KCl, respectively. Arrest is defined as a pause that lasts longer than 20 min or until the tether breaks. Data for transcription of bare DNA are in black; nucleosome data are in semitranslucent colors. The shaded region represents the NPS.

dian pause duration from 4.3 s on bare DNA to 8.1 s at the nucleosome. Thus, the nucleosome slows the underlying pause recovery mechanism of the polymerase. Finally, pause-free velocity at the NPS was reduced from 17.5 ± 2 bp s^{-1} on bare DNA to 10.5 ± 3 bp s^{-1} in the presence of a nucleosome (Fig. 2C) (*8*).

Many transcriptional pauses of Pol II on bare DNA are associated with backtracking of the enzyme along the DNA template (*10*–*12*). Pauses end when the polymerase diffusively realigns the dislocated 3′ end of the transcript with its active site and resumes elongation. The probability density of pause durations, $\psi(t)$, is equivalent to the distribution of first-passage times for return to the origin of a Poisson stepper that takes integral steps along a one-dimensional lattice (*13*, *14*), and is given by

$$\psi(t) = \sqrt{\frac{k_f}{k_b}}\,\frac{\exp[-(k_f + k_b)t]}{t}\,I_1\left(2t\sqrt{k_f k_b}\right) \quad (1)$$

where I_1 is the modified Bessel function of the first kind, and k_f and k_b are the forward and backward stepping rates, respectively, during a backtrack (Fig. 3). These rates depend on force according to

$$k_f = k_0 \exp\left(\frac{Fd}{k_B T}\right) \quad (2)$$

$$k_b = k_0 \exp\left(-\frac{Fd}{k_B T}\right) \quad (3)$$

where k_0 is the intrinsic zero-force stepping rate of Pol II diffusion along DNA during a backtrack, F is the force, and d is the distance to the transition state for a step (taken here to be 0.5 bp). For small forces, $\psi(t)$ reduces to the $t^{-3/2}$ power-law dependence previously reported (*10*). We maintained the applied force between 4 and 8 pN at the NPS and fit the cumulative distribution corresponding to $\psi(t)$ to the pause durations on bare DNA to determine $k_0 = 0.33 \pm 0.05$ s^{-1} (Fig. 2B); thus, our data confirm that pause recovery occurs through a diffusive mechanism that is slow relative to elongation.

A backtracked polymerase cannot actively separate downstream nucleosomal DNA from the surface of the histones because it possesses no energy source. Moreover, the DNA downstream of a backtracked polymerase can stochastically rewrap around the histones, restricting Pol II from diffusing back to the 3′ end of the nascent RNA to resume transcription, thereby increasing pause durations. Because local nucleosomal fluctuations are fast relative to the diffusive stepping rate k_0 (*15*), the nucleosome reaches fast local equilibrium between each backtracking step. Thus, we expect pause durations on nucleosomal DNA to be drawn from the same distribution as on bare DNA, but with a net forward stepping rate reduced by a factor corresponding to the fraction of time the local nucleosomal DNA is unwrapped, $\gamma_u = k_u/(k_u + k_w)$, where k_w and k_u are the rates of local wrapping and unwrapping of the DNA around the histones, respectively:

$$k_{f(nucl)} \rightarrow k_f \gamma_u \quad (4)$$

Using the value of k_0 determined above, the cumulative distribution of pause durations in the presence of a nucleosome at 300 mM KCl is correctly fit by the diffusive backtracking model when $\gamma_u = 0.48 \pm 0.05$, indicating that nucleosomal DNA is locally unwrapped half of the time immediately downstream of a polymerase.

During active transcription, forward elongation competes kinetically with pausing. Therefore, the increased pause density at a nucleosome can be used to infer changes in the net elongation rate, allowing us to discriminate between two possible scenarios: one in which Pol II can elongate only against a locally unwrapped nucleosome (Fig. 3), and another in which the polymerase can advance by actively unwrapping nucleosomal DNA (fig. S11). We first examine the predictions of the model where Pol II passively waits for unwrapping fluctuations of the nucleosome (Fig. 3). Here, pause density at the nucleosome has a similar form as on bare DNA, except with a dependence on γ_u (*8*):

$$P_{\text{bare DNA}} = \frac{k_b}{k_b + k_e} \quad (5)$$

$$P_{\text{nucleosome}} = \frac{k_b}{k_b + \gamma_u k_e} \quad (6)$$

We are able to verify the net irreversible elongation rate k_e by fitting the observed pause density on bare DNA to the above expression; we find $k_e = 16 \pm 5$ s^{-1}, in agreement with our measurements of pause-free velocity (Fig. 2C). Using this value of k_e, along with the values of k_b and γ_u obtained above, the model predicts a nucleosomal pause density of 0.017 ± 0.006 bp^{-1} for pauses longer than 2 s, a number that matches well our experimental measurements (Fig. 2A).

The alternative scenario, in which the polymerase can actively open a wrapped nucleosome and elongate through it with a rate $k_{e,w}$ (fig. S11), predicts a smaller pause density (*8*):

$$P_{\text{nucleosome, active unwrapping}} = \frac{k_b}{k_b + \gamma_u k_e + (1 - \gamma_u)k_{e,w}} \quad (7)$$

This prediction does not fit the observed peak value in pause density (above 0.02 bp^{-1}) unless $k_{e,w} = 0$ s^{-1}, which simplifies to the scheme shown in Fig. 3.

Local wrapping of the nucleosome prevents elongation, and because these nucleosomal fluctuations are very fast, the associated transcriptional delays are below the temporal resolution of our instrument. Instead, they have an impact on the apparent pause-free velocity of Pol II, reducing it to $k_e^{app} = \gamma_u k_e$ (*8*). Using our measurement of pause-free velocity on bare DNA (17.5 ± 2 bp s^{-1}), the model predicts an apparent pause-free velocity on nucleosomal DNA of 8.4 ± 1 bp s^{-1}, in close

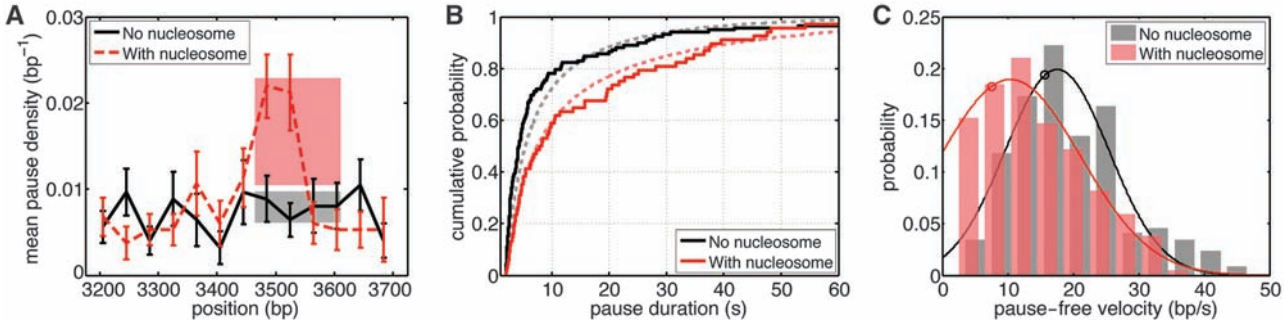

Fig. 2. Effect of the nucleosome on transcription dynamics. In each plot, only traces that passed the NPS are considered. (**A**) Pause density with a nucleosome (dashed red line) and on bare DNA (solid black line). The pink shaded area represents the pause density confidence interval at the nucleosome as predicted from the model presented in the text. The gray shaded region is the confidence interval for pause density on bare DNA used in the model. Error bars are SEM. (**B**) Cumulative distributions of pause durations with (solid red line) and without (solid black line) a nucleosome present. Theoretical cumulative distributions are shown for nucleosomal (pink dashed line) and non-nucleosomal (gray dashed line) pauses. (**C**) Pause-free velocities with (pink) and without (gray) a nucleosome with fits to normal distributions (solid lines). The predicted values based on the diffusive model with and without a nucleosome are shown as red and black circles, respectively.

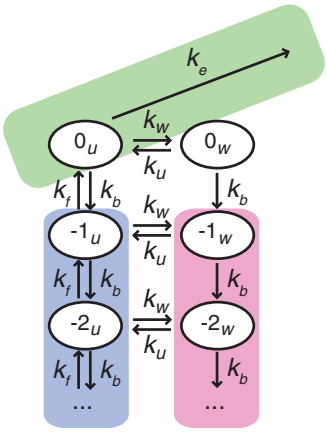

Fig. 3. Kinetic model of transcription through a nucleosome. The green area corresponds to on-pathway elongation (k_e). The pink and blue areas represent off-pathway paused states where Pol II is backtracked; negative numbers indicate how many bases Pol II has backtracked from the elongation competent state, denoted by 0. The subscript u refers to the nucleosome being locally unwrapped (blue area); w denotes the states where the nucleosome is wrapped in front of Pol II (pink area).

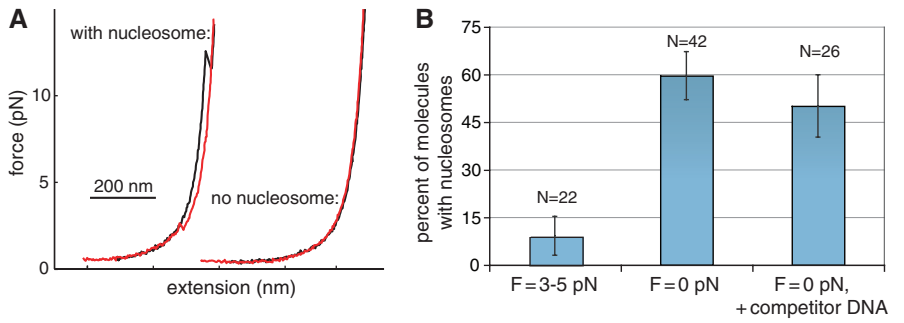

Fig. 4. Histone transfer during transcription. (**A**) Force-extension curves of transcribed DNA. Pulling curves are shown in black and relaxation curves in red. (**B**) Frequency of histone transfer as a function of applied force during transcription.

agreement with our experimental measurement of 10.5 ± 3 bp s^{-1} (Fig. 2C). Thus, during both backtracking and elongation, Pol II does not actively unwrap nucleosomal DNA, but instead waits for fluctuations that locally unwrap the nucleosome to advance, consistent with ratcheting mechanisms proposed for transcription elongation (*16*, *17*).

It has been proposed that a transient DNA loop (*18*, *19*) might allow the histones of a partially unwrapped nucleosome to contact DNA behind the polymerase and remain associated with the DNA after transcription (*2*, *4*, *5*, *18*). The probability of forming such a thermally induced DNA loop should be sensitive to forces as low as 0.2 pN (*20*). We designed a construct that stops the polymerase in a mechanically stable conformation after it has passed the nucleosome (*8*); this strategy allowed us to obtain force-extension curves of the transcribed DNA to determine the dependence of histone transfer on applied force.

We monitored transcription of the nucleosomal region at forces between 3 and 5 pN, then pulled on the transcribed DNA when Pol II reached the end of the template. Very few molecules displayed nucleosome unwrapping transitions (2 of 22) despite marked pausing at the NPS; instead, most showed monotonic force-extension curves, indicating that no nucleosome was present behind the polymerase (Fig. 4A). In contrast, when transcription proceeded in bulk before tether formation so that the DNA template was not under tension during transcription, a significant fraction of complexes showed nucleosomes upstream of the polymerase (25 of 42, $P < 0.0001$), indicating that histone transfer had occurred (Fig. 4B). Histone transfer was not significantly affected by an eightfold excess (50 ng/μl) of competitor DNA (13 of 26, $P < 0.0025$), a concentration sufficient to capture displaced histones (*18*). We conclude that histones are transferred in cis to DNA upstream of Pol II upon nucleosomal transcription, as the looping model proposes, and that tension inhibits formation of the looped intermediate necessary for transfer. This interpretation is consistent with the reduction in pause density as the polymerase advances through the NPS (Fig. 2A), because either the histones detach from the DNA, are transferred to DNA upstream of the enzyme, or are pushed to a lower-affinity (i.e., higher γ_u) downstream sequence.

Regulation of elongation and pausing is of great importance for cotranscriptional processes such as alternative splicing (*21*, *22*). Indeed, a large number of genes from different species are regulated during elongation by extended pausing, including many important developmental and heat shock–induced genes (*23*–*29*). Because nucleosomes are located at ubiquitous, well-defined positions in the genome and act as general repressors of transcription, they constitute a potential scaffold for the regulation of transcription elongation. Our study indicates that modulation of the wrapping/unwrapping equilibrium of DNA around the histone octamer constitutes the physical basis for regulation of transcription through nucleosomal DNA.

References and Notes

1. M. G. Izban, D. S. Luse, *Genes Dev.* **5**, 683 (1991).
2. M. L. Kireeva *et al.*, *Mol. Cell* **9**, 541 (2002).
3. W. Walter, M. L. Kireeva, V. M. Studitsky, M. Kashlev, *J. Biol. Chem.* **278**, 36148 (2003).
4. M. L. Kireeva *et al.*, *Mol. Cell* **18**, 97 (2005).
5. V. A. Bondarenko *et al.*, *Mol. Cell* **24**, 469 (2006).
6. R. M. Widmer *et al.*, *EMBO J.* **3**, 1635 (1984).
7. C. Thiriet, J. J. Hayes, *Genes Dev.* **19**, 677 (2005).
8. See supporting material on *Science* Online.
9. C. Bustamante, J. F. Marko, E. D. Siggia, S. Smith, *Science* **265**, 1599 (1994).
10. E. A. Galburt *et al.*, *Nature* **446**, 820 (2007).
11. N. Komissarova, M. Kashlev, *Proc. Natl. Acad. Sci. U.S.A.* **94**, 1755 (1997).
12. N. Komissarova, M. Kashlev, *J. Biol. Chem.* **272**, 15329 (1997).
13. W. Feller, *An Introduction to Probability Theory and Its Applications* (Wiley, New York, ed. 2, 1971), vol. 2, pp. 59–65.
14. M. Depken, E. A. Galburt, S. W. Grill, *Biophys. J.* **96**, 2189 (2009).
15. G. Li, M. Levitus, C. Bustamante, J. Widom, *Nat. Struct. Mol. Biol.* **12**, 46 (2004).
16. P. H. von Hippel, E. Delagoutte, *Cell* **104**, 177 (2001).
17. G. Bar-Nahum *et al.*, *Cell* **120**, 183 (2005).
18. V. M. Studitsky, D. J. Clark, G. Felsenfeld, *Cell* **76**, 371 (1994).
19. V. M. Studitsky, G. A. Kassavetis, E. P. Geiduschek, G. Felsenfeld, *Science* **278**, 1960 (1997).
20. J. Yan, R. Kawamura, J. F. Marko, *Phys. Rev. E* **71**, 061905 (2005).
21. G. Nogues, S. Kadener, P. Cramer, D. Bentley, A. R. Kornblihtt, *J. Biol. Chem.* **277**, 43110 (2002).
22. M. de la Mata *et al.*, *Mol. Cell* **12**, 525 (2003).
23. A. E. Rougvie, J. T. Lis, *Cell* **54**, 795 (1988).
24. A. Krumm, T. Meulia, M. Brunvand, M. Groudine, *Genes Dev.* **6**, 2201 (1992).
25. L. J. Strobl, D. Eick, *EMBO J.* **11**, 3307 (1992).
26. A. Plet, D. Eick, J. M. Blanchard, *Oncogene* **10**, 319 (1995).
27. D. L. Bentley, M. Groudine, *Nature* **321**, 702 (1986).
28. S. A. Brown, A. N. Imbalzano, R. E. Kingston, *Genes Dev.* **10**, 1479 (1996).
29. L. J. Core, J. T. Lis, *Science* **319**, 1791 (2008).

30. We thank E. Galburt, Y. Zhang, and M. Kireeva for helpful advice, as well as D. King, J. Choy, and S. Grill for technical assistance, and J. Wittmeyer for her gift of plasmids for histone proteins. Supported by NIH grant GM32543 (C.B.).

Supporting Online Material

www.sciencemag.org/cgi/content/full/325/5940/626/DC1
Materials and Methods
SOM Text
Figs. S1 to S13
References

2 March 2009; accepted 16 June 2009
10.1126/science.1172926